

CHARACTERISTICS OF ELECTROMAGNETIC SYSTEMS OF MAGNETIC BEARINGS BIASED WITH PERMANENT MAGNETS

Satoru Fukata,¹ Kazuyuki Yutani²

ABSTRACT

Two electromagnetic systems interact each other in the active magnetic radial bearings that are combined with permanent magnets to provide bias force and electromagnets to supply control force. The characteristics are studied when a single electromagnet system is excited by a sinusoidal input with fixed working airgap. The frequency characteristics of incremental fluxes are measured in the exciting and non-exciting magnetic systems. The experimental results are compared with the numerical results based on an analysis, to check the validity of the analysis giving a deeper understanding of the complicated magnetic systems.

INTRODUCTION

A combination of electromagnets and permanent magnets has been considered to construct active magnetic bearings (Boden and Scheffer, 1968, 1972; NASA, 1974; Allaire et al., 1990; AVCON, Inc.). A simple and compact structure of the bearings is the sharing of magnet pole legs with the electromagnets and the permanent magnets. This structure is similar in appearance to the all electromagnetic design with homopolar geometry; however, the construction of magnetic circuits is different. The electromagnetic flux flowing out of a pole leg passes through a rotor core radially and enters an opposing pole leg. Hence, the two flux paths in the horizontal and vertical directions cross in the rotor core. This fact leads to complicated characteristics of the magnetic systems with interactions.

About the analysis of those interacting magnetic systems, Allaire et al. (1990) presented a basic approach to the static characteristics, using the magnetic circuit theory. Lee et al. (1994) gave a more elaborate analysis with the measurement of static magnetic forces. For the dynamic characteristics, Fukata and Yutani (1997) presented a simple linearized model with variations of working airgap, using the circuit theory with the demagnetization curve of permanent magnets.

The present paper shows experimental results of the dynamic characteristics with fixed working airgap, and gives the comparison with the numerical results based on the analysis.

¹Department of Engineering Design, Kyushu Institute of Design, 4-9-1 Shiobaru, Minami-ku, Fukuoka 815-8540, Japan.

²Department of Mechanical Engineering, Kyushu Institute of Technology, 1-1 Sensui-cho, Tobata-ku, Kitakyushu 804-8550, Japan.

For three cases of rotor position, we excite a single electromagnet system with a sinusoidal input, and measure the frequency characteristics of incremental magnetic fluxes in the exciting and non-exciting pole legs. The experimental results are compared with numerical results based on the analysis, to check its validity and to give a deeper understanding of the complicated magnetic systems.

MAGNETIC SYSTEM

Figure 1 illustrates the construction and main flux paths of radial magnetic bearings composed of permanent magnets for biasing and electromagnets for control. Four axially magnetized permanent segments are positioned circumferentially between two stator rings. The permanent magnetic flux passes through the laminated stator pole leg, the working airgap and the rotor axially, then returns to the permanent magnet via a pole leg of the other stator ring.

The electromagnet coils installed on the radially opposing pole legs are connected in series together with those of the other stator rings and are driven by a single power amplifier. The electromagnetic flux passes down the stator pole leg, through the working gap and the rotor radially, and enters the radially opposing pole leg. The return flux takes two paths along the stator ring, as shown in Fig. 1. Thus, the total flux increases on one side of the rotor and decreases on the other side. The electromagnetic flux paths in the horizontal direction are omitted in the figure.

Since the distribution of bias magnetic flux is determined by the magnetic resistances, we may give an effective distribution with different sizes in pole legs. Taking larger ones in the vertical direction than in the horizontal direction, we can compensate a decrease in bias flux, due to a bias current of the electromagnet, on the lower side. We may use the permanent magnetic flux more effectively to suspend a part of the dead weight of the rotor by setting larger ones on the upper side than on the lower side. The magnet coils on one of the two stator rings may be removed if unnecessary as in Allaire et al. (1990).

We number the pole legs and the working airgaps with ij by $i=1, 2$ to the left- and right-hand stator-rings, respectively; $j=1, 2$ to the lower and upper sides, $j=3, 4$ to the left- and right-hand sides, respectively, in each stator. The permanent magnets and the associated flux paths are numbered by j in the same way as above. The magnet system is referred to 1 for the vertical direction and 3 for the horizontal direction. These numbers will be used in the subscript to show the associated variables and constants.

EXPERIMENTAL RESULTS WITH FIXED WORKING AIRGAP

EXPERIMENTAL SETUP

Figure 2 shows the mechanical part of the experimental set up of the radial magnetic bearing. The two stator rings are of equal dimensions. The pole legs are of the same size of 10mm all in axial thickness and 12mm in width in the horizontal direction and on the lower side in the vertical direction. The width of the upper-side pole legs is 15.6mm, 30% wider than that of the others, to supply a larger permanent magnetic flux to suspend a part of the deadweight of the rotor. The winding of electromagnet coil is 100 turns in each pole leg.

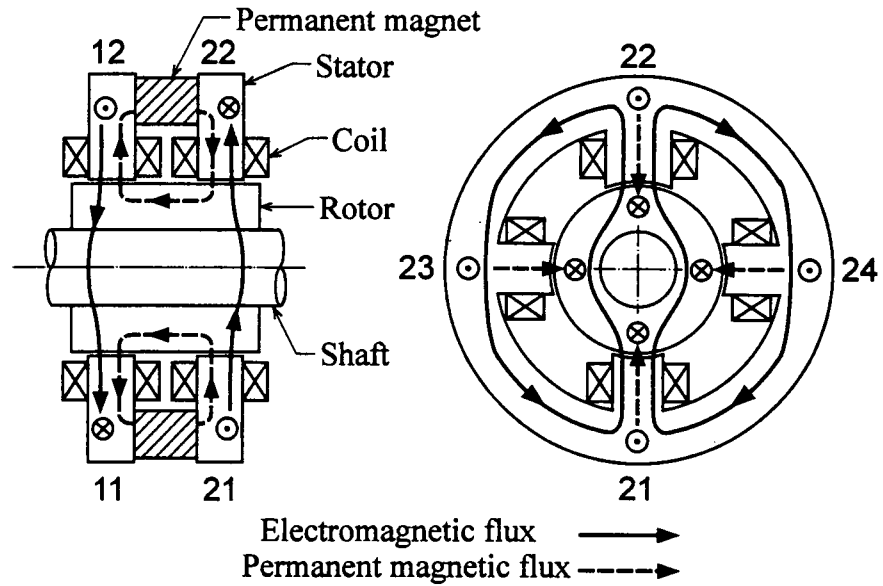


Figure 1 Construction and main flux paths of radial magnetic bearing.

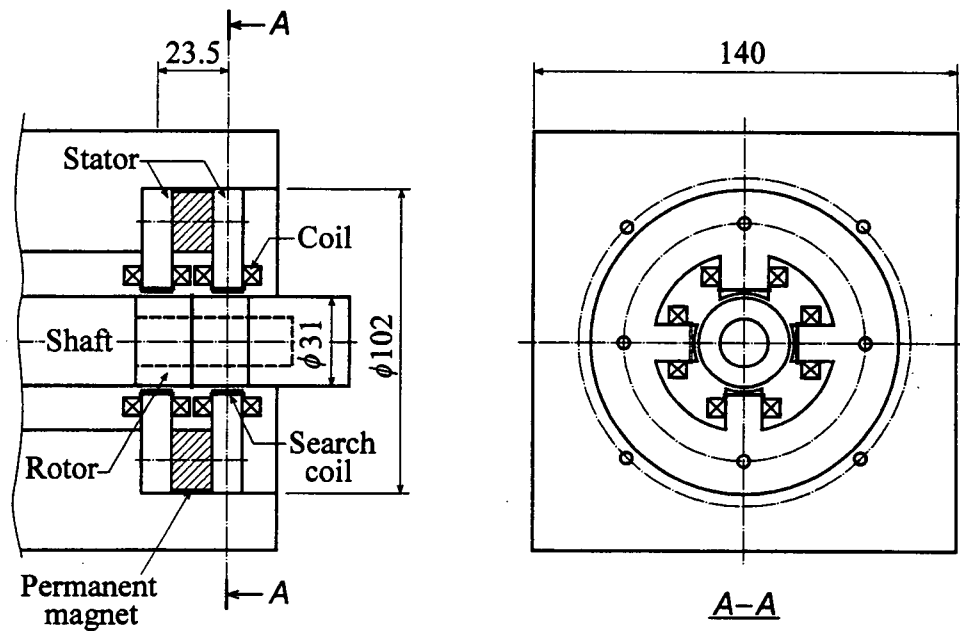


Figure 2 Experimental setup.

The stator and rotor cores are made of silicon steel strips of 0.2mm thickness. The permanent magnetic flux path interconnecting the two rotor cores may be made of solid iron; here we used the silicon steel strips, for simplicity. The stator rings have the outer and inner diameters of 102mm and 60mm, respectively. The rotor core in the shape of a ring is 31mm and 16mm in the outer and inner diameters, respectively, and is guided on a shaft of aluminum. The single biasing permanent magnets are composed of three pieces of ferrite and 13.5mm in total thickness; each piece has the residual magnetic flux density of 0.36T

according to its opened characteristics.

We fixed the working airgaps by paper, and excited the electromagnet system of the vertical direction in three cases of rotor position.

- (1) The rotor is centered, i.e., the working airgap lengths are set all to the nominal value of 0.6mm.
- (2) The rotor is moved up by a half of the nominal airgap length, i. e., the working airgap lengths are 0.3mm and 0.9mm on the upper and lower vertical sides, respectively, and the nominal value in the horizontal direction.
- (3) The rotor is further shifted onto the left- or right-hand side by a half of the nominal length.

We express the increments with the following symbols, and their Laplace transforms using their upper case with Laplace operator s .

e_1 : input voltage to power amplifier of the electromagnet

i_1 : coil current of the electromagnet

ϕ_{1j} : incremental flux in pole leg $1j$ ($\phi_{1j} = \phi_{2j}$)

ϕ_R : incremental flux axially passing through the rotor and over the two stator rings

CHARACTERISTICS OF COIL CURRENT

In measuring frequency characteristics, we applied a non-biasing sinusoidal input voltage of an amplitude of 0.6V to the power amplifier. We guess that this amplitude generates a static flux increment of about 45% of the biasing permanent magnetic flux in the nominal working airgap length.

In Experiment (1) with the nominal airgap, the frequency response of the magnet coil current was approximated in very good agreement with the that of the transfer function

$$\frac{I_1(s)}{E_1(s)} = 0.91 \frac{e^{-0.02s}}{0.09s + 1}, \quad s : 1/\text{ms} \quad (1)$$

In Experiment (2), we had a similar good approximation by replacing the time constant 0.09 ms with 0.10ms. This small dependence of the time constant on the rotor position is a property of the electromagnet system of a pair of opposing magnet coils.

FREQUENCY CHARACTERISTICS OF ELECTROMAGNETIC FLUX

We wound search coils of two turns on pole legs near their pole face to measure the incremental fluxes ϕ_{1j} . The axial incremental flux ϕ_R was detected through a search coil on the rotor between the two rotor cores. We first obtained the frequency responses of generating voltage in the search coils, and then applied numerical integral operation to them.

In Experiment (1) the frequency responses to the input voltage are shown by the filled lines in Fig. 3 for the exciting magnet pole legs, and in Fig. 4 for the others. The phase of ϕ_{12} is omitted, which is similar to that of ϕ_{11} . The frequency responses in Experiment (2) are given in Figs. 5 and 6 by the filled lines. The responses in Experiment (3), which are omitted here, were statically different from, but dynamically similar to those in Experiment (2).

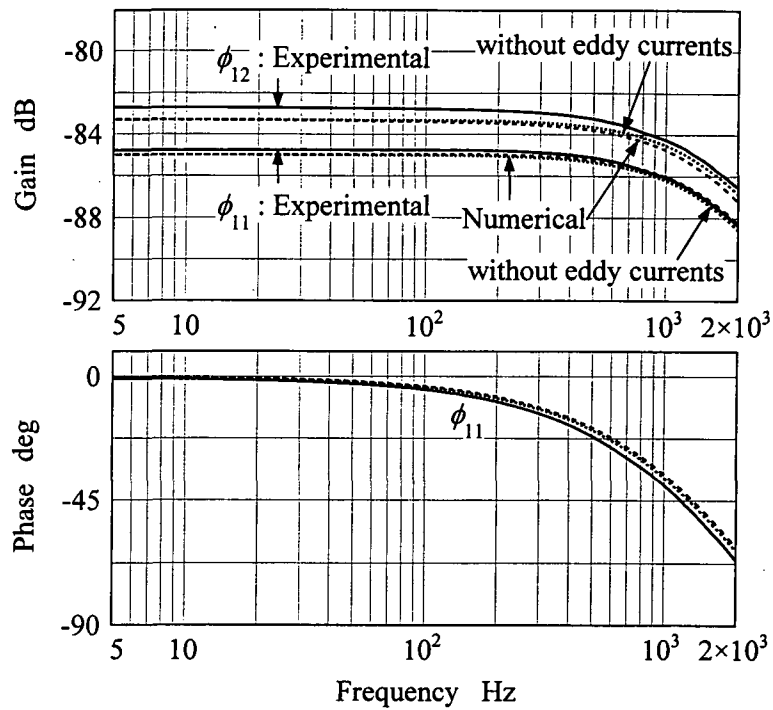


Figure 3 Frequency responses of incremental fluxes in exciting pole legs. The rotor is centered with nominal working airgap of 0.6mm.

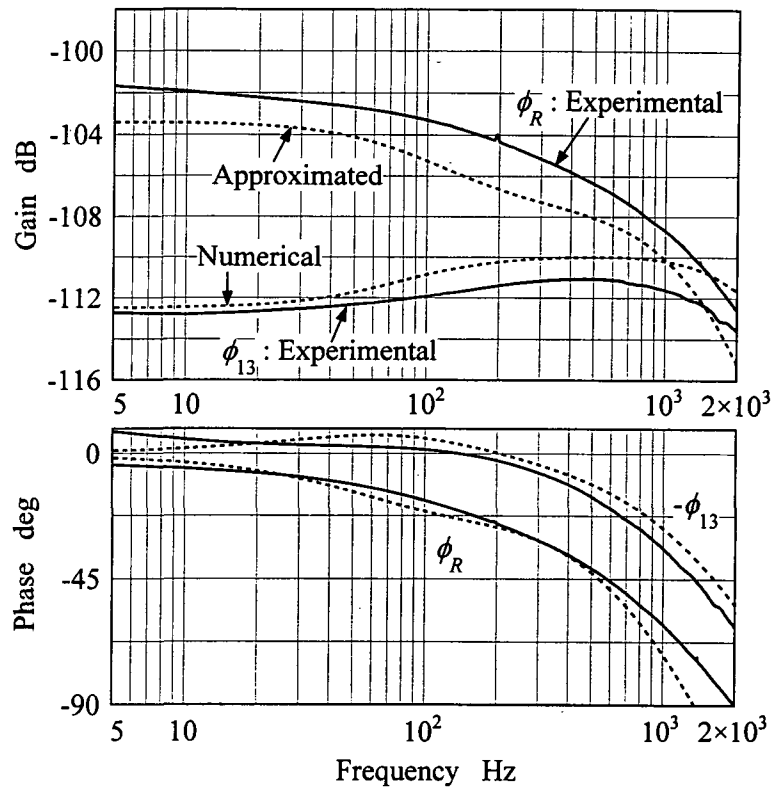


Figure 4 Frequency responses of incremental fluxes in non-exciting pole leg and rotor. The rotor is centered with nominal working airgap of 0.6mm.

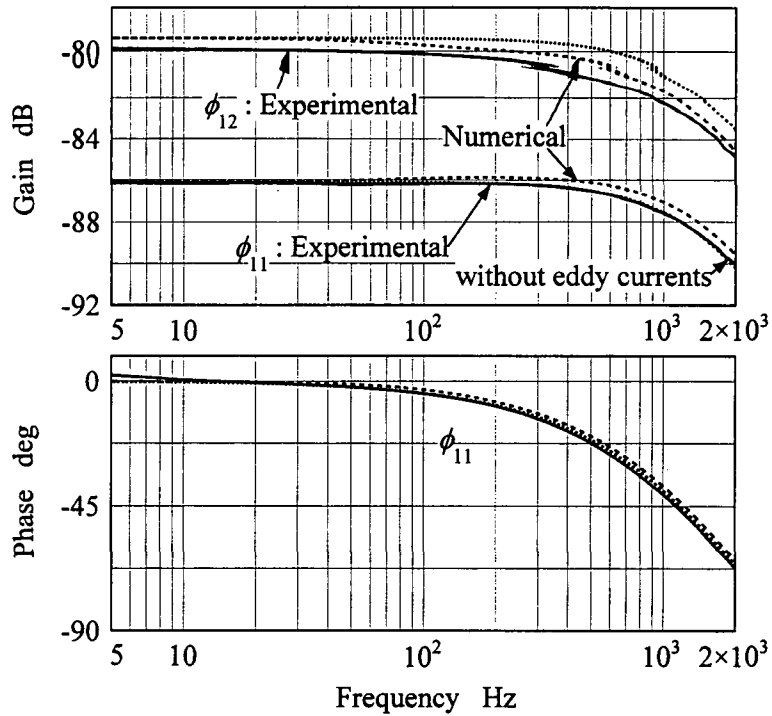


Figure 5 Frequency responses of incremental fluxes in exciting pole legs. The rotor is shifted by 0.3mm upward.

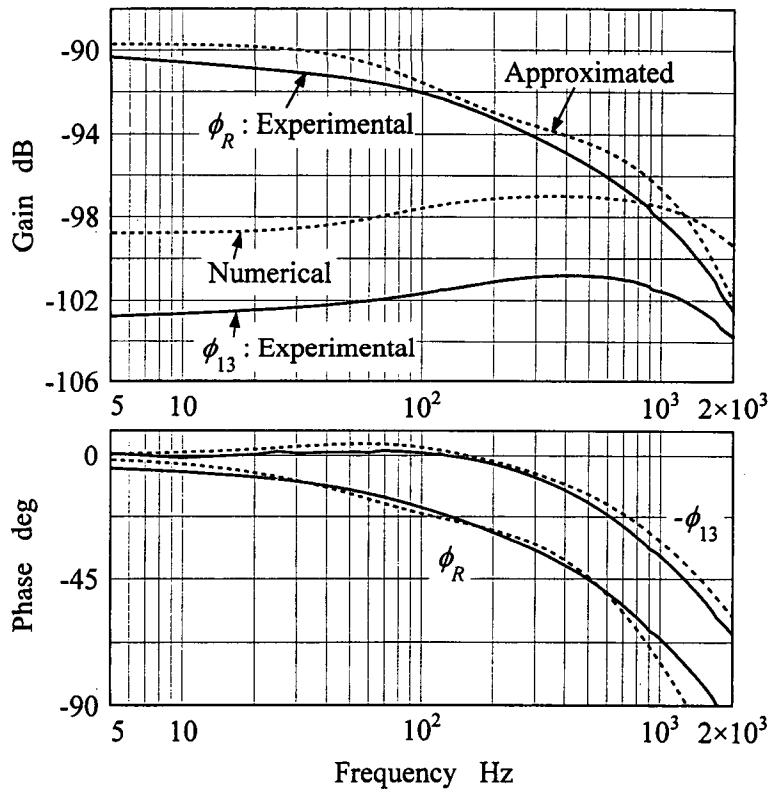


Figure 6 Frequency responses of incremental fluxes in non-exciting pole leg and rotor. The rotor is shifted by 0.3mm upward.

The experimental results show the following properties.

- (1) The incremental fluxes on the opposing sides are not equal in general (we note that the upper-side pole leg is larger than that of the lower side).
- (2) A part of the difference, about a half in lower frequencies, passes through the rotor axially and returns through the space between the two stator rings. This bypass flux decreases with increasing frequency.
- (3) A part of the difference takes another shortcut through the non-exciting pole legs. This bypass flux increases with frequency.

In the above item (2), the decrease in the axial bypass flux is due to the eddy current effects. The effects give an increase in the magnetic resistance of the non-laminated axial path with exciting frequency. A part of flux excluded from this path takes another shortcut passing through the non-exciting pole legs. This is the reason of the latter part in the item (3).

NUMERICAL ANALYSIS

ANALYTICAL RESULTS

Fukata and Yutani (1997) analyzed the magnetic system in Fig.1 under several conditions. They presented linearized expressions for the incremental magnetic fluxes with variations of the rotor position. If the working airgaps are fixed, then we obtain a simpler form without those conditions, provided that there is no magnetic saturation. We use the following symbols.

- N : turns of electromagnet coil on single pole leg
- R_{1j0} : magnetic resistance associated with working airgap $1j$ ($R_{1j0} = R_{2j0}$)
- R_{10} : parallel resistance of R_{1j0} , $j = 1, 2, 3, 4$
- R_R, R_S : axial magnetic resistance in rotor, between two stator rings
- R_T : series resistance of R_{10} , R_{20} , R_R and R_S

Instead of the incremental magnetic fluxes, we use the variables defined by

$$q_{1j} = \frac{R_{1j0}}{N} \phi_{1j}, \quad j = 1, 2, 3, 4; \quad q_R = \frac{R_T}{N} \phi_R \quad (2)$$

These variables are dynamically equivalent to the magnetic fluxes, and have the unit of current. For our experimental setup, we have the following relations with transfer functions.

$$\frac{Q_{1j}(s)}{I_1(s)} = \beta_{1j} + (-1)^{j-1} \alpha_{10} g_{RS}(s), \quad j = 1, 2 \quad (3)$$

$$-\frac{Q_{13}(s)}{I_1(s)} = \frac{Q_{14}(s)}{I_1(s)} = \gamma_{110} + \alpha_{10} g_{RS}(s) = \gamma_{110} \frac{\tilde{T}_{2e1}' s^2 + \tilde{T}_{1e1}' s + 1}{\tilde{T}_{2e} s^2 + \tilde{T}_{1e} s + 1} \quad (4)$$

$$\frac{Q_R(s)}{I_1(s)} = \gamma_{10} + g_{RS}(s) = \gamma_{10} \frac{T_{2e} s^2 + T_{1e} s + 1}{\tilde{T}_{2e} s^2 + \tilde{T}_{1e} s + 1} \quad (5)$$

$$g_{RS}(s) = \gamma_{10} \frac{\tau_{2e}s^2 + \tau_{1e}s}{\tilde{T}_{2e}s^2 + \tilde{T}_{1e}s + 1} \quad (6)$$

where

$$\alpha_{10} = \frac{R_{10}}{R_T}, \quad \alpha_{1j0} = \frac{R_{10}}{R_{1j0}}, \quad \bar{\alpha}_{112} = \alpha_{110} - \alpha_{120},$$

$$\beta_{11} = 1 - \gamma_{110}, \quad \beta_{12} = 1 + \gamma_{110},$$

$$\gamma_{10} = 2\bar{\alpha}_{112}, \quad \gamma_{110} = (1 - 2\alpha_{10})\bar{\alpha}_{112} \quad (7)$$

$$\tilde{T}_{2e} = T_{2e} + \tau_{2e}, \quad \tilde{T}_{1e} = T_{1e} + \tau_{1e},$$

$$\tilde{T}_{2e1}' = \tilde{T}_{2e} + \frac{\gamma_{10}}{\gamma_{110}} \alpha_{10} \tau_{2e}, \quad \tilde{T}_{1e1}' = \tilde{T}_{1e} + \frac{\gamma_{10}}{\gamma_{110}} \alpha_{10} \tau_{1e} \quad (8)$$

and where

$$\frac{1}{R_{10}} = \sum_{j=1}^4 \frac{1}{R_{1j0}}, \quad R_T = 2R_{10} + R_R + R_S \quad (9)$$

The transfer function $g_{RS}(s)$ of eq. (6) is a low-order approximation of eddy current effects in the axial flux path. The time constants are unknown and to be identified in general.

We estimate the magnetic resistance with

$$R_{1j0} = \frac{l_{m1j}}{\mu_0 A_{1j}}, \quad A_{1j} = (H + 2l)(W + 2l)_{1j} \quad (10)$$

where H and W are the axial and circumferential widths, respectively, of the pole leg face, the term $2l$ is the fringing effect in the working airgap of length l , l_{m1j} the equivalent airgap length considering the magnetic resistance in the cores, and μ_0 the permeability of air.

It seems difficult to correctly estimate the axial magnetic resistances in the rotor and stator rings, R_R and R_S ; hence we assume them using the ratio λ_{RS} with

$$R_R + R_S = \lambda_{RS}(R_{R0} + R_{S0}) \quad (11)$$

where R_{R0} and R_{S0} are estimated from a simple equation similar to eq. (10) for the mean axial-path length without fringing effect.

We take a value of 5,000 for the relative permeability of the magnet cores, and 0.93 for the stacking factor of the lamination in calculating the axial magnetic resistances.

STATIC GAINS

We consider the gains at 10Hz the experimental static gains for the comparison with the numerical analysis (we see that there seem to be some errors in the low frequencies). They are

shown in the left part of **Table I**.

Under some assumptions for the bypass magnetic resistances, the static gains of the incremental fluxes are calculated as in Table I from eqs. (1) to (5). From these results, we draw the conclusions:

- (1) The calculation leads to an erroneous result for the exciting system when neglecting the interaction to the other system and the axial bypass flux. Considering them improves the results.
- (2) The magnetic resistance in the axial bypath has a small effect on the values of the exciting system, but a large effect on the values of the non-exciting system and axial bypath.
- (3) Our calculation is unsatisfactory to the non-exciting system in Experiments (2) and (3). The calculation gives much larger values.

FREQUENCY RESPONSES

We obtain the frequency responses to an input voltage with the static gains calculated with $\lambda_{RS}=0.5$, which are shown in the right-hand side of Table I. Without eddy current effects in the axial bypath, i.e., $g_{RS}(s) = 0$, the results are shown in Figs. 3 and 5 by the dotted lines.

To consider the eddy current effects, we approximate the frequency characteristics of the axial bypass flux with eq. (4). In Experiment (1), we obtain the transfer function

$$\frac{Q_R(s)}{I_1(s)} = \gamma_{10} \left(\frac{0.6}{0.1s + 1} + \frac{0.4}{1.5s + 1} \right), \quad s : 1/\text{ms} \quad (12)$$

TABLE I STATIC GAINS OF INCREMENTAL FLUXES TO INPUT VOLTAGE

		Airgap [mm]	Measured at 10Hz [dB]	Calculated [dB]			
				$\lambda_{RS} = \infty$ $\phi_{13} = \phi_{14} = 0$	$\lambda_{RS} = \infty$ ($R_S = \infty$)	$\lambda_{RS} = 1$ $\xi = 0.93$	$\lambda_{RS} = 0.5$ $\xi = 0.93$
(1)	ϕ_{11}	0.6	-84.8 (1.00)	-83.9	-84.3 (1.00)	-84.5 (1.00)	-84.6 (1.00)
	ϕ_{12}	0.6	-82.7 (1.27)	-83.9	-83.3 (1.13)	-83.1 (1.17)	-83.0 (1.19)
	$\phi_{13} = \phi_{14}$	0.6	-112.8 (0.04)	0	-108.1 (0.06)	-110.6 (0.05)	-112.5 (0.04)
	ϕ_R	-	-101.9 (0.14)	0	0 (0)	-107.5 (0.07)	-103.4 (0.11)
(2)	ϕ_{11}	0.9	-86.2 (1.00)	-83.9	-85.2 (1.00)	-85.7 (1.00)	-86.0 (1.00)
	ϕ_{12}	0.3	-79.9 (2.07)	-83.9	-80.8 (1.65)	-80.0 (1.92)	-79.5 (2.11)
	$\phi_{13} = \phi_{14}$	0.6	-102.6 (0.15)	0	-94.9 (0.33)	-97.1 (0.27)	-98.8 (0.23)
	ϕ_R	-	-90.6 (0.60)	0	0 (0)	-94.0 (0.38)	-89.7 (0.65)
(3)	ϕ_{11}	0.9	-86.1 (1.00)	-83.9	-85.4 (1.00)	-85.8 (1.00)	-86.1 (1.00)
	ϕ_{12}	0.3	-79.7 (2.09)	-83.9	-80.5 (1.76)	-79.8 (2.00)	-79.4 (2.16)
	ϕ_{13}	0.9	-103.7 (0.13)	0	-98.4 (0.22)	-100.4 (0.19)	-102.0 (0.16)
	ϕ_{14}	0.3	-98.8 (0.23)	0	-90.7 (0.54)	-92.7 (0.45)	-94.3 (0.39)
	ϕ_R	-	-90.5 (0.60)	0	0 (0)	-94.6 (0.36)	-90.2 (0.62)

The values in parentheses give the ratios to ϕ_{11}

i. e., $T_{2e} = 0$, $T_{1e} = 0.94\text{ms}$, $\bar{T}_{2e} = 0.15(\text{ms})^2$ and $\bar{T}_{1e} = 1.6\text{ms}$. This frequency response with eq. (1) is plotted in Fig. 4 by broken lines. With these time constants, we have the numerical frequency responses as given by broken lines in Figs. 3 and 4.

In a similar way in Experiment (2), we have a similar approximation with 1.8ms instead of 1.5ms in the second term of eq. (12), and we have $T_{2e} = 0$, $T_{1e} = 1.12\text{ms}$, $\bar{T}_{2e} = 0.18(\text{ms})^2$ and $\bar{T}_{1e} = 1.9\text{ms}$. The approximated response and the calculated responses are shown by the broken lines in Figs. 5 and 6.

We see that the dynamical characteristics of the numerical analysis are in good agreement with those of the experiments. We may conclude that the eddy current effects of the axial path are negligible in practice on the exciting magnet system.

CONCLUSIONS

We studied the characteristics of the electromagnet systems of radial magnetic bearings biased with permanent magnets, with fixed working airgaps. We confirmed that the two magnet systems in the radial direction interact each other, in general. We also see that there is an axial flux bypassing through the rotor and the space between the two stator rings, decreasing with the eddy current effects in higher frequencies. We compared the experimental results with the numerical results based on the analysis presented before, to check its validity. We may conclude that the eddy current effects in the axial path are small on the main fluxes.

We thank Nippon Steel Corporation for supplying us silicon steel strips.

REFERENCES

- Allaire, P. E. et al. 1990. "Permanent Magnet Biased Magnetic Bearings-Design, Construction, and Testing," *Proc. 2nd Inter. Sympo. Magnetic Bearings*, Tokyo:175-182.
- AVCON Inc. Catalogues on Magnetic Bearings.
- Boden, K. and D. Scheffer. 1968. "Magnetische Lagerung," German Patent 1750602 with supplements 1933031, 1967085, 1967086, US patent 3,650,581.
- Boden, K. and D. Scheffer. 1972. "Elektromagnetisches Lagerelement," German patent 2213465, US patent 3,877,761.
- Lee, A. C., F. Z. Hsiao, and D. Ko. 1994. "Analysis and Testing of a Magnetic Bearing with Permanent Magnets for Bias," *JSME Int. Journal*, C-37(4):774-782.
- Fukata, S., and K. Yutani. 1997. "Analysis of Magnetic systems of Magnetic Bearings Biased with Permanent Magnets," *Memoirs of Fac. Engg., Kyushu University*, 57(1):17-35.
- NASA. 1974. "Magnetic Bearings with Combined Radial and Axial Control," *NASA Tech. Brief*, B74-10131.